

Detecting Wandering Intermediate-Mass Black Holes with AXIS in the Milky Way and Local Massive Galaxies

Fabio Pacucci^{1,2†}, Bryan Seepaul¹, Yueying Ni¹, Nico Cappelluti³, and Adi Foord⁴

¹ Center for Astrophysics | Harvard & Smithsonian, 60 Garden St., Cambridge MA, 02138

² Black Hole Initiative at Harvard University, 20 Garden St., Cambridge MA, 02138

³ University of Miami

⁴ Department of Physics, University of Maryland Baltimore County, 1000 Hilltop Cir, Baltimore, MD 21250, USA

† Email: fabio.pacucci@cfa.harvard.edu

Abstract: This white paper explores the detectability of intermediate-mass black holes (IMBHs) in the Milky Way (MW) and in massive local galaxies, with a particular emphasis on the role of AXIS. IMBHs, ranging within $10^3\text{--}6\text{ }M_{\odot}$, are commonly found at the centers of dwarf galaxies and may exist, yet undiscovered, in the MW. By using model spectra for advection-dominated accretion flows (ADAFs), we calculated the expected fluxes emitted by a population of wandering IMBHs with a mass of $10^5\text{ }M_{\odot}$ in various MW environments and extrapolated our results to massive local galaxies. Around 40%, in number, of the potential population of wandering IMBHs in the MW can be detected in an AXIS deep field. We proposed criteria to aid in the selection of IMBH candidates using already-available optical surveys. We also showed that IMBHs wandering in > 200 galaxies within 10 Mpc can be easily detected with AXIS when passing within dense galactic environments (e.g., molecular clouds and cold neutral medium). In summary, we highlighted the potential X-ray detectability of wandering IMBHs in local galaxies and provided insights for guiding future surveys. Detecting wandering IMBHs is crucial for understanding their demographics, evolution, and the merging history of galaxies. *This White Paper is part of a series commissioned for the AXIS Probe Concept Mission; additional AXIS White Papers can be found at [some url].*

Contents

1	Introduction	3
2	Detecting Wandering IMBHs in the X-rays with AXIS	3
2.1	Accretion rates and spectral energy distributions	3
2.2	X-ray observability and selection criteria: the role of AXIS	4
2.3	Extending the search to local galaxies	5
3	Concluding Remarks	6
	References	6

List of Figures

- 1 **Left panel:** distribution of accretion rates, categorized in the five ISM environments investigated. All rates are strongly sub-Eddington. **Right panel:** collection of SEDs for five values of the accretion rate representative of each ISM environment. 4
- 2 **Left panel:** Probability density of the X-ray fluxes produced by IMBHs passing through the five ISM environments considered. The AXIS flux limit is indicated. **Right panel:** Luminosity ratios (optical to X-ray, and sub-mm to optical) for the selection of IMBH candidates in multi-wavelength surveys. 5
- 3 X-ray fluxes ($0.2 - 10$ keV) generated by the passage of a $10^5 M_{\odot}$ IMBH as a function of its distance. The green-shaded area is detectable by an AXIS deep field. Electromagnetic signatures of the passage of an IMBH can be detected in MC and CNM in more than 200 external galaxies within 10 Mpc. 6

1. Introduction

Many of the black holes (BHs) observed thus far are accreting at or near the Eddington rate $\dot{M}_{\text{Edd}} \approx 1.4 \times 10^{18} M_{\bullet} \text{ g s}^{-1}$, where M_{\bullet} is the mass of the compact object in solar masses. In this limiting case, the outward acceleration on a test particle resulting from radiation pressure is balanced by the inward gravitational acceleration. Notably, this is the case of high-luminosity quasars, characterized by super-massive BHs with masses $M_{\bullet} > 10^6 M_{\odot}$. In the conventional α -disk model [25,39], $\sim 10\%$ of the rest-mass energy (Mc^2) of infalling material is radiated away [21].

This standard picture of accretion has been widely tested, especially in the high- z Universe [6], where the large availability of gas makes accretion at the Eddington rate feasible [32]. However, the radiative efficiency, ϵ , can significantly deviate from the typical 10% value, both for strongly super-Eddington ($\dot{M} \gg \dot{M}_{\text{Edd}}$) and sub-Eddington ($\dot{M} \ll \dot{M}_{\text{Edd}}$) accretion rates [2,4,28,36,43].

Below 1% of the Eddington rate, the advection-dominated accretion flow (ADAF) regime is entered [1,20,22,23,46]. BHs accreting in the ADAF mode exhibit radiative efficiencies several orders of magnitude lower than the typical $\sim 10\%$ value. Given the rarity of conditions supporting large accretion rates in the local Universe, it is likely that a substantial fraction of BHs accretes in the ADAF mode, including the super-massive BH at the center of the MW [47]. Similarly, a putative population of intermediate-mass BHs (IMBHs) wandering in galaxies would also accrete in ADAF mode.

IMBHs are a bridge between stellar mass and super-massive objects and have masses in the range $10^3 M_{\odot} < M_{\bullet} < 10^6 M_{\odot}$, although the definition greatly varies depending on the sub-field of interest. IMBHs have been extensively detected in dwarf galaxies in accordance with scaling relations [15], and have active fractions from $\sim 5\%$ to 22% [10,27]. Recent studies are investigating the existence of wandering IMBHs in the MW and massive galaxies and their orbital and radiative properties [5,34,44,45].

IMBHs potentially wandering in the MW could have formed (i) in situ and (ii) ex situ. In situ (i.e., within the galaxy) formation channels include super-Eddington accretion onto stellar-mass BHs [35], direct collapse of high-mass quasi-stars [37,41], runaway mergers in dense globular stellar clusters [8,12,31,40], and supra-exponential accretion on seed black holes in the early universe [3,24]. The ex-situ channel forms them in the nucleus of a satellite/dwarf that merged with the more massive galaxy [9,11,26,42].

These wandering IMBHs accrete from the interstellar medium (ISM) at low rates $\dot{M} \ll \dot{M}_{\text{Edd}}$, resulting in electromagnetic signatures typical of ADAF accretion mode. A recent study [38] modeled the accretion and radiation properties of IMBHs of $10^5 M_{\odot}$ wandering in the MW, using five realistic ISM environments [7]: molecular clouds (MCs), cold neutral medium (CNM), hot neutral medium (HNM), warm ionized medium (WIM), and hot ionized medium (HIM). The mass of the perturbing black hole was chosen as the typical mass of IMBHs detected in the nuclei of dwarfs [10]. The accretion rate onto the IMBH was estimated using a Bondi rate, properly adjusted to account for outflows and convection [13,29,33,38].

This white paper first summarizes the result presented in [38], focusing on the X-ray properties of wandering IMBHs in the MW. Then, expands on the contribution that AXIS could provide to detecting these sources. Lastly, it makes predictions for the observability of IMBHs wandering in local galaxies.

2. Detecting Wandering IMBHs in the X-rays with AXIS

2.1. Accretion rates and spectral energy distributions

The left panel of Fig. 1 displays the distribution of accretion rates predicted for a $10^5 M_{\odot}$ IMBH wandering in typical ISM environments of the MW. The accretion rates span ~ 10 orders of magnitude, from 10^{-14} to $10^{-4} M_{\odot} \text{ yr}^{-1}$. MC and CNM environments show the largest accretion rates because they are the densest; as such, they offer the best changes for an X-ray detection of IMBHs in the MW.

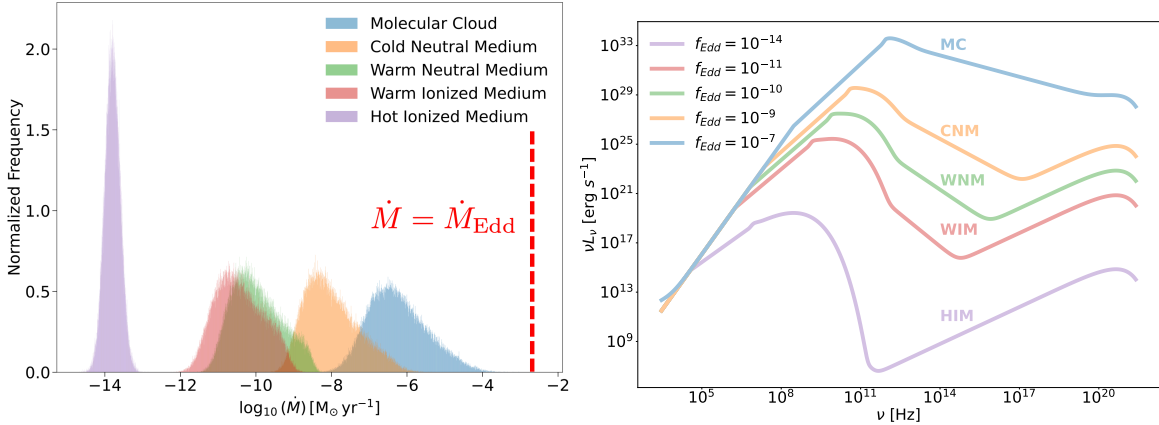


Figure 1. Left panel: distribution of accretion rates, categorized in the five ISM environments investigated. All rates are strongly sub-Eddington. **Right panel:** collection of SEDs for five values of the accretion rate representative of each ISM environment.

Note that the Eddington rate on an IMBH of 10^5 M_{\odot} is $\dot{M}_{\text{Edd}} \approx 2 \times 10^{-3} \text{ M}_{\odot} \text{ yr}^{-1}$: all accretion rates predicted are strongly sub-Eddington. The resulting spectral energy distributions (SED) are shown in the right panel of Fig. 1, with Eddington ratios (defined as the accretion rate normalized to the Eddington rate) ranging from 10^{-11} to 10^{-3} . The SEDs were computed using a code specifically designed for compact objects accreting in ADAF mode [30]. The peak of the SED shifts to higher frequencies with increasing accretion rates.

2.2. X-ray observability and selection criteria: the role of AXIS

The left panel of Fig. 2 displays the resulting volume-weighted flux distribution in the X-ray part of the spectrum. These results suggest that AXIS, in its proposed deep survey [18,19] with a flux limit $\sim 3 \times 10^{-18} \text{ erg s}^{-1} \text{ cm}^{-2}$ and an area of 0.1 deg^{-2} , will detect a fraction, in number, of $\sim 38\%$ of wandering IMBHs in the MW, assuming a uniform sampling of the region occupied by the Galaxy (see also the AXIS white paper by Cappelluti et al. 2023).

To aid in the task of selecting IMBH candidates, [38] proposed basic selection criteria to be employed in photometric surveys. The right panel of Fig. 2 shows two luminosity ratios calculated as a function of the Eddington ratio of the IMBH: (i) the X-ray to optical/UV ratio represented by the standard α_{ox} parameter [17], and (ii) the optical/UV to sub-mm ratio (see [38] for their definition). A combination of X-ray, optical, and sub-mm observations can sift out potential candidates and uniquely determine the accretion rate onto wandering IMBHs.

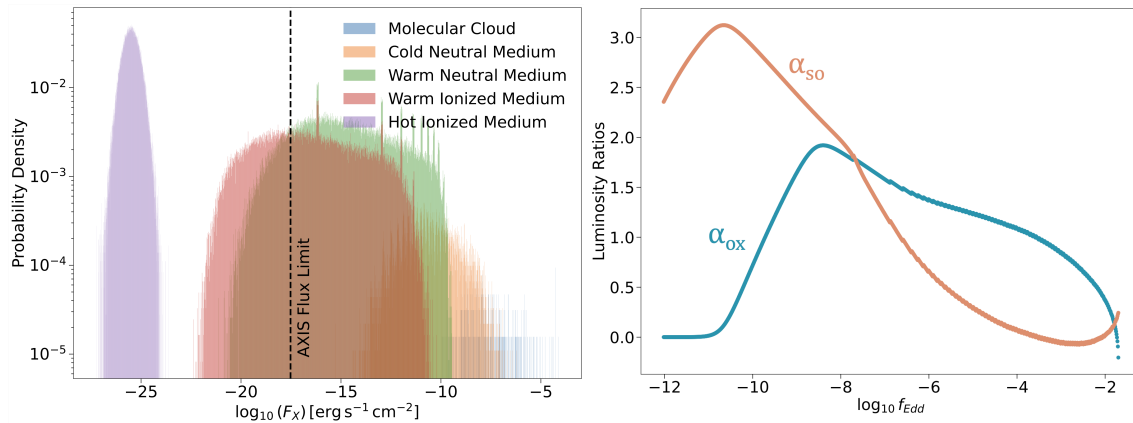


Figure 2. **Left panel:** Probability density of the X-ray fluxes produced by IMBHs passing through the five ISM environments considered. The AXIS flux limit is indicated. **Right panel:** Luminosity ratios (optical to X-ray, and sub-mm to optical) for the selection of IMBH candidates in multi-wavelength surveys.

Predicting the number of IMBHs detectable by AXIS in a deep Galactic survey is challenging because the total number of such sources is unknown. The MW has encountered $\sim 15 \pm 3$ galaxies with a stellar mass $> 10^7 M_\odot$ during its cosmic evolution [16]. Such galaxies could have hosted IMBHs that are massive enough to be detected in AXIS searches. Hence, assuming an expected number of ~ 10 IMBHs, [44] showed that these objects are more likely to wander in the innermost ~ 1 kpc of the MW. It is, nonetheless, informative to compare its capabilities with other currently operational facilities. Table 1 shows that AXIS would allow a significant improvement of at least 40% over current facilities, thanks not only to its extraordinary sensitivity but also its wide field of view.

Table 1. Volume-weighted detectability of wandering IMBHs of $10^5 M_\odot$ in the MW by AXIS, Chandra, and eROSITA. The detectability indicates the percent of the total number of such objects that are detectable by a given instrument.

X-ray telescope	Flux limit [$\text{erg s}^{-1} \text{cm}^{-2}$]	Detectability
AXIS	3.0×10^{-18}	38%
Chandra	2.0×10^{-16}	27%
eRosita	2.0×10^{-14}	13%

2.3. Extending the search to local galaxies

The left panel of Fig. 2 shows that the passage of a $10^5 M_\odot$ IMBH generates the highest X-ray fluxes within MCs and CNM environments. Galaxies in the same mass category of the MW share a similar environmental composition. Hence, we investigate the fluxes that the passage of equally massive IMBHs would produce in nearby galaxies.

In Fig. 3, we show the X-ray fluxes (0.2 – 10 keV) generated by the passage of a $10^5 M_\odot$ IMBH in the five ISM environments, for a range of distances between 1 kpc and 10 Mpc. We indicate the distance to a few example locations, from the Galactic center to the Andromeda galaxy, noting that within a radius of 4 Mpc there are more than 200 galaxies [14]. We calculated the flux reported in Fig. 3 for the five ISM environments from their *median luminosity*. As some environments exhibit a range of luminosities spanning ~ 13 orders of magnitudes (see Fig. 2), the typical values of fluxes in Fig. 3 are indicative.

From Fig. 3, we gather that the median luminosity generated in the WNM, WIM, and HIM are invisible to AXIS or detectable only within the MW. On the contrary, fluxes generated in the CNM and

MCs are detectable by an AXIS deep field well outside the MW. AXIS imaging reaching a depth of $\sim 3 \times 10^{-18} \text{ erg s}^{-1} \text{ cm}^{-2}$ could detect the electromagnetic signature of the passage of an IMBH of $10^5 M_\odot$ in well over 200 galaxies within 10 Mpc distance. Although MCs and CNM environments occupy only a small volume fraction of a typical MW-like galaxy (0.05% and 1%, respectively, see [7]), the availability of a large number of external galaxies within reach greatly expands the chances of detecting such signatures.

As most of the X-ray luminosities of the sources considered here are $< 10^{40} \text{ erg s}^{-1}$, contamination from X-ray binaries (XRB) is of concern. To disentangle their emission, synergies with observatories in other wavelengths (e.g., JWST, Roman, and Rubin) will be fundamental.

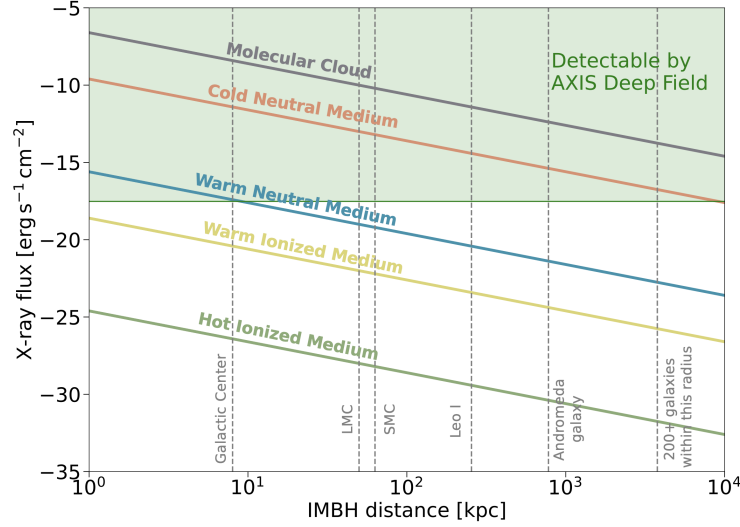


Figure 3. X-ray fluxes (0.2 – 10 keV) generated by the passage of a $10^5 M_\odot$ IMBH as a function of its distance. The green-shaded area is detectable by an AXIS deep field. Electromagnetic signatures of the passage of an IMBH can be detected in MC and CNM in more than 200 external galaxies within 10 Mpc.

3. Concluding Remarks

To conclude, AXIS represents a significant improvement over current X-ray facilities and opens up the way to detect a completely unknown population of black holes. Both in the MW and, even more crucially, in > 200 local galaxies, AXIS is able to detect the X-rays emitted by the passage of IMBHs within dense ISM environments. Such detections are crucial for understanding the demographics and evolution of IMBHs, and the merging history of galaxies.

Acknowledgments: F.P. acknowledges support from a Clay Fellowship administered by the Smithsonian Astrophysical Observatory. This work was also supported by the Black Hole Initiative at Harvard University, which is funded by grants from the John Templeton Foundation and the Gordon and Betty Moore Foundation. We kindly acknowledge the AXIS team for their outstanding scientific and technical work over the past year. This work is the result of several months of discussion in the AXIS-AGN SWG.

References

1. Abramowicz, M. A., Chen, X., Kato, S., Lasota, J.-P., & Regev, O. 1995, *ApJ*, **438**, L37
2. Abramowicz, M. A., Czerny, B., Lasota, J. P., & Szuszkiewicz, E. 1988, *ApJ*, **332**, 646
3. Alexander, T., & Natarajan, P. 2014, *Science*, **345**, 1330
4. Begelman, M. C. 1978, *MNRAS*, **184**, 53
5. Di Matteo, T., Ni, Y., Chen, N., et al. 2022, *arXiv e-prints*, arXiv:2210.14960
6. Fan, X., Banados, E., & Simcoe, R. A. 2022, *arXiv e-prints*, arXiv:2212.06907
7. Ferrière, K. M. 2001, *Reviews of Modern Physics*, **73**, 1031

8. González, E., Kremer, K., Chatterjee, S., et al. 2021, [ApJ](#), 908, L29
9. Governato, F., Colpi, M., & Maraschi, L. 1994, [MNRAS](#), 271, 317
10. Greene, J. E., Strader, J., & Ho, L. C. 2020, [ARA&A](#), 58, 257
11. Greene, J. E., Lancaster, L., Ting, Y.-S., et al. 2021, [ApJ](#), 917, 17
12. Gürkan, M. A., Freitag, M., & Rasio, F. A. 2004, [ApJ](#), 604, 632
13. Igumenshchev, I. V., Narayan, R., & Abramowicz, M. A. 2003, [ApJ](#), 592, 1042
14. Karachentsev, I. D., Makarov, D. I., & Kaisina, E. I. 2013, [AJ](#), 145, 101
15. Kormendy, J., & Ho, L. C. 2013, [Annual Review of Astronomy and Astrophysics](#), 51, 511
16. Kruijssen, J. M. D., Pfeffer, J. L., Chevance, M., et al. 2020, [MNRAS](#), 498, 2472
17. Lusso, E., Comastri, A., Vignali, C., et al. 2010, [A&A](#), 512, A34
18. Marchesi, S., Gilli, R., Lanzuisi, G., et al. 2020, [A&A](#), 642, A184
19. Mushotzky, R., Aird, J., Barger, A. J., et al. 2019, in [Bulletin of the American Astronomical Society](#), Vol. 51, 107
20. Narayan, R., & McClintock, J. E. 2008, [New A Rev.](#), 51, 733
21. Narayan, R., & Quataert, E. 2005, [Science](#), 307, 77
22. Narayan, R., & Yi, I. 1994, [ApJ](#), 428, L13
23. —. 1995, [ApJ](#), 452, 710
24. Natarajan, P. 2021, [MNRAS](#), 501, 1413
25. Novikov, I. D., & Thorne, K. S. 1973, in [Black Holes \(Les Astres Occlus\)](#), 343
26. O’Leary, R. M., Kocsis, B., & Loeb, A. 2009, [MNRAS](#), 395, 2127
27. Pacucci, F., Mezcu, M., & Regan, J. A. 2021, [ApJ](#), 920, 134
28. Paczynski, B., & Abramowicz, M. A. 1982, [ApJ](#), 253, 897
29. Perna, R., Narayan, R., Rybicki, G., Stella, L., & Treves, A. 2003, [ApJ](#), 594, 936
30. Pesce, D. W., Palumbo, D. C. M., Narayan, R., et al. 2021, [ApJ](#), 923, 260
31. Portegies Zwart, S. F., & McMillan, S. L. W. 2002, [ApJ](#), 576, 899
32. Power, C., Baugh, C. M., & Lacey, C. G. 2010, [MNRAS](#), 406, 43
33. Proga, D., & Begelman, M. C. 2003, [ApJ](#), 592, 767
34. Ricarte, A., Tremmel, M., Natarajan, P., & Quinn, T. 2021, [ApJ](#), 916, L18
35. Ryu, T., Tanaka, T. L., Perna, R., & Haiman, Z. 2016, [MNRAS](#), 460, 4122
36. Sadowski, A. 2009, [ApJS](#), 183, 171
37. Schleicher, D. R. G., Palla, F., Ferrara, A., Galli, D., & Latif, M. 2013, [A&A](#), 558, A59
38. Seepaul, B. S., Pacucci, F., & Narayan, R. 2022, [MNRAS](#), 515, 2110
39. Shakura, N. I., & Sunyaev, R. A. 1973, [A&A](#), 500, 33
40. Shi, Y., Grudić, M. Y., & Hopkins, P. F. 2021, [MNRAS](#), 505, 2753
41. Volonteri, M., & Begelman, M. C. 2010, [MNRAS](#), 409, 1022
42. Volonteri, M., Haardt, F., & Madau, P. 2003, [ApJ](#), 582, 559
43. Volonteri, M., & Rees, M. J. 2005, [ApJ](#), 633, 624
44. Weller, E. J., Pacucci, F., Hernquist, L., & Bose, S. 2022, [MNRAS](#), 511, 2229
45. Weller, E. J., Pacucci, F., Ni, Y., et al. 2023, [MNRAS](#), 520, 3955
46. Yuan, F., & Narayan, R. 2014, [ARA&A](#), 52, 529
47. Yuan, F., Quataert, E., & Narayan, R. 2003, [ApJ](#), 598, 301